

Transfer Coefficients of Momentum, Heat and Water Vapour in the Atmospheric Surface Layer of a Large Freshwater Lake

Wei Xiao · Shoudong Liu · Wei Wang ·
Dong Yang · Jiaping Xu · Chang Cao ·
Hanchao Li · Xuhui Lee

Received: 28 November 2012 / Accepted: 2 May 2013 / Published online: 30 May 2013
© Springer Science+Business Media Dordrecht 2013

Abstract In studies of lake–atmosphere interactions, the fluxes of momentum, water vapour and sensible heat are often parametrized as being proportional to the differences in wind, humidity and air temperature between the water surface and a reference height above the surface. Here, the proportionality via transfer coefficients in these relationships was investigated with the eddy-covariance method at three sites within an eddy-covariance mesonet across Lake Taihu, China. The results indicate that the transfer coefficients decreased with increasing wind speed for weak winds and approached constant values for strong winds. The presence of submerged macrophytes reduced the momentum transfer (drag) coefficient significantly. At the two sites free of submerged macrophytes, the 10-m drag coefficients under neutral stability were $1.8 (\pm 0.4) \times 10^{-3}$ and $1.7 (\pm 0.3) \times 10^{-3}$ at the wind speed of 9 m s^{-1} , which are 38 and 34 % greater than the prediction by the Garratt model for the marine environment.

Keywords Eddy covariance · Evaporation · Lake Taihu · Sensible heat · Submerged macrophytes · Transfer coefficients

1 Introduction

Lakes are an important land-surface type for atmospheric research. There are 304 million lakes in the world, covering 4.2 million km^2 or 4 % land area (Downing et al. 2006). Even though this fraction appears small, it is important to society for the reason that many large

W. Xiao (✉) · S. Liu · W. Wang · D. Yang · J. Xu · C. Cao · H. Li · X. Lee
Yale-NUIST Center on Atmospheric Environment, Nanjing University of Information Science
& Technology, Nanjing 210044, Jiangsu, China
e-mail: xiaowei_522@163.com

X. Lee (✉)
School of Forestry and Environmental Studies, Yale University, 21 Sachem Street,
New Haven, CT 06511, USA
e-mail: xuhui.lee@yale.edu

municipalities are located near lake shorelines. With different albedo, higher heat capacity, and lower roughness length than the surrounding land area, lakes tend to influence the local climate through lake–land-breeze circulations (Samuelsson and Tjernström 2001; Törnblom et al. 2007; Sills et al. 2011) and through the alteration of precipitation (Samuelsson et al. 2010; Zhao et al. 2012). Lake–atmosphere interactions are driven by the fluxes of momentum, sensible heat and water vapour between the water surface and the atmosphere. In many numerical weather prediction and climate models, the surface fluxes of momentum, sensible heat and water vapour form the lower boundary conditions for the equations governing atmospheric flow and heat and water budgets and are parametrized using bulk transfer relationships (Henderson-Sellers 1986; Oleson et al. 2004; Subin et al. 2012). The transfer coefficients are taken from experimental studies conducted in open oceans (e.g. Garratt 1992), and there are few experimental studies on their applicability to lake environments.

Lakes differ from the oceans in several respects: first, it is known that water depth is a factor controlling the interaction between lake systems and the atmosphere (MacKay et al. 2009). For example, wave height—a critical parameter affecting the drag coefficient—may be limited by water depth (especially shallow water bodies) and fetch in lake systems whereas in the open ocean it is dependent mostly on fetch (Geernaert et al. 1987; Smith et al. 1992; Donelan et al. 1993; Ataktürk and Katsaros 1999; Panin et al. 2006; Gao et al. 2009). Second, wind speed above inland lakes is generally lower than over the open ocean, and can fall outside the range of experimental conditions under which the transfer coefficient parametrizations were established. Third, submerged macrophytes are common in shallow lake systems (e.g. Pip 1979; Johnson and Ostrofsky 2004; Radomski and Perleberg 2012). Shallow lakes are defined by the Minnesota Pollution Control Agency as “lakes with a maximum depth of 4.6 m or less, or with 80 % or more of the lake area shallow enough to support emergent and submerged rooted aquatic plants.” Among the 3254 lakes in Minnesota studied by Radomski and Perleberg (2012), 71 % lakes are shallow, with at least 51 % of the lake area less than 4.6 m in depth. The growing depth of submerged macrophytes ranges from 0.3 to 24 m according to data for over 700 European lakes (Søndergaard et al. 2013). Even though these plants are known to reduce the turbulent mixing within the lake water (Carpenter and Lodge 1986; Losee and Wetzel 1993; Nepf 1999; Vermaat et al. 2000; Madsen et al. 2001; Herb and Stefan 2005; Plew et al. 2008), little research has been carried out on their role on lake–air exchange processes. Although lake–air fluxes of momentum, heat and water vapour have been reported in several lake experimental studies (e.g. Heikinheimo et al. 1999; Blanken et al. 2000, 2003, 2011; Schertzer et al. 2003; Liu et al. 2005, 2009; Vesala et al. 2006; Rouse et al. 2008; Nordbo et al. 2011), we are not aware of studies that have evaluated the relationships of the transfer coefficients to these lake biophysical attributes.

We have recently launched an observational program on in-situ measurements of the fluxes of momentum, heat and masses using the eddy-covariance method across Lake Taihu, China (Fig. 1). In this paper, we aim to quantify the dependence of the transfer coefficients on wind speed and the effect of submerged macrophytes. Our results are interpreted in the context of the transfer coefficient values inferred from the lake studies cited above and the standard parametrizations for the marine environment (Garratt 1992). The data used in this study came from three eddy-covariance sites on the lake, two of which were in water free of macrophytes and one was surrounded with submerged macrophytes. Our long data records (6–24 months) covered a wide range of wind and stability conditions. Because of the large data size, our estimation of the transfer coefficients should be less prone to random measurement errors than those studies published from short field campaigns.

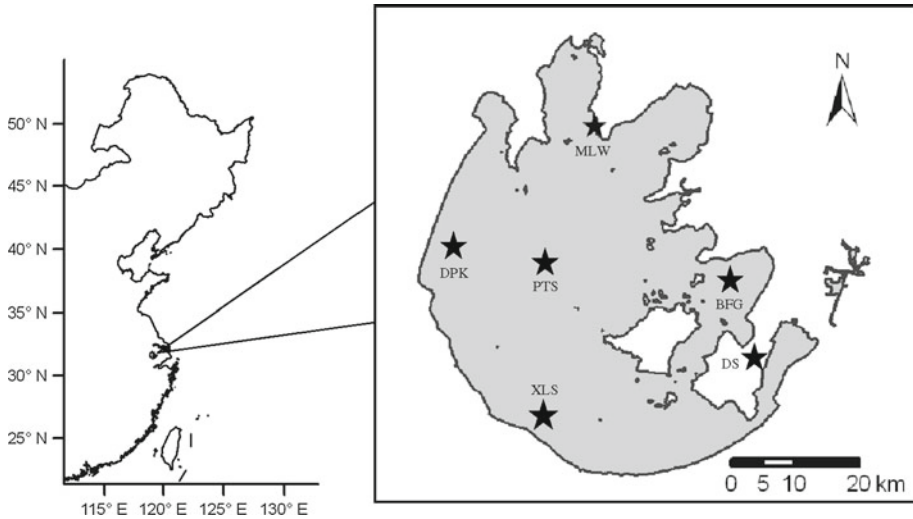


Fig. 1 Map showing the eddy-flux mesonet measurement sites at Lake Taihu. This study used the data obtained at the MLW (Meiliangwan), DPK (Dapukou) and BFG (Bifenggang) sites. The two other lake sites—PTS (Pingtaishan) and XLS (Xiaoleishan)—were established in November 2012 and do not have long enough data records for inclusion in this analysis

2 Methods

2.1 Sites and Instruments

The experiment was conducted at three sites in the Taihu Eddy Flux Mesonet (Fig. 1); the sites differed in their distance to the shoreline and in the influence of submerged macrophytes. Bifenggang site (BFG, 120°24'E, 31°10'N) was located in the east part of Lake Taihu, where submerged macrophytes (mainly *Potamogeton malaianus* and *Hydrilla verticillata*) dominated the aquatic ecosystem (Fig. 2). Dapukou (DPK, 119°56'E, 31°16'N) and Meiliangwan (MLW, 31°24'N, 120°13'E) sites were located in the western and northern parts of Lake Taihu, respectively, where phytoplankton (e.g. *Microcystis aeruginosa*, *Anabaena flos-aquae*, *Aulacoseira granulate*, *Cryptomonas* spp., *Scenedesmus bijuga* and *Pediastrum duplex*, Chen et al. 2003) was abundant and no submerged macrophyte was present. Lake Taihu is the third largest freshwater lake in China, with a water surface area of 2,400 km² and mean water depth of 1.9 m. The DPK site was in the deeper portion of the lake where the annual mean water depth was 2.6 m.

An eddy-correlation system and a set of micrometeorological sensors were mounted on a fixed platform at the BFG and DPK sites and on a concrete pillar at the MLW site in the lake. At the BFG site, a three-dimensional sonic anemometer/thermometer (model CSAT3, Campbell Scientific Inc., Logan, UT, USA) and an open-path infrared gas analyzer (model EC150, Campbell Scientific Inc., Logan, UT, USA) were employed to measure the three-dimensional wind speed, air temperature, and atmospheric water vapour and CO₂ concentrations at 10 Hz. Fluxes of momentum (τ), sensible heat (H) and latent heat ($L_v E$) were computed using block averaging from the 10 Hz time series over 30-min intervals. The EC measurement height was 8.45, 8.50 and 3.54 m above the water surface at the BFG, DPK and MLW sites, respectively. A net radiometer (model CNR4, Kipp & Zonen B.V., Delft, The Netherlands) was used to



Fig. 2 Submerged macrophytes in the lake at the BFG site

measure the four components of the surface radiation balance (incoming shortwave, reflected shortwave, incoming longwave and outgoing longwave radiation). A temperature and relative humidity probe (model HMP155A, Vaisala Inc. Helsinki, Finland) and a wind monitor (model 05103, R M Young Company, Traverse City, Michigan, USA) were used to measure air temperature and relative humidity, wind speed and wind direction. Water temperature at 0.20, 0.50, 1.00 and 1.50 m depths and temperature of the lake sediment were measured using temperature probes (model 109-L, Campbell Scientific Inc., Logan, Utah, USA). The instruments at the DPK and MLW sites were of the same type as the BFG site except for the open-path infrared gas analyzer (model LI7500, Li-Cor Inc., Lincoln, Nebraska, USA).

The eddy-correlation and meteorological measurements commenced on 15 December 2011 at the BFG site, on 18 August 2011 at the DPK site and on 14 June 2010 at the MLW site. We used the data collected from the commencement dates to 30 June 2012 and for wind directions in the range of 135–315° at the BFG site, 100–280° at the DPK site and 200–315° at the MLW site. The corresponding linear distance to the shoreline was greater than 3, 2 and 8 km at the BFG, DPK and MLW sites, respectively. The peak contribution to the flux footprint was 230, 230 and 90 m away from the measurement location for the BFG, DPK and MLW sites, respectively, in neutral stability according to the footprint model of [Hsieh et al. \(2000\)](#). In these direction ranges the sonic anemometers suffered least interference from the instrument-mounting hardware. Measurements affected by precipitation were also excluded. In all, 8.8, 4.7 and 4.3% data were excluded due to precipitation, and 56, 40 and 78% data were excluded due to poor fetch for the BFG, DPK and MLW sites, respectively. The data were post-processed with a coordinate rotation into the natural wind coordinate ([Lee et al. 2004](#)), using a water vapour density correction to the sonic temperature and a density correction to the water vapour flux ([Webb et al. 1980](#); [Lee and Massman 2011](#)).

2.2 Data Analysis

The analysis is based on the bulk transfer relationships

$$\tau = \rho_a C_D u^2, \quad (1)$$

$$L_v E = \rho_a L_v C E u (q_s - q_a), \quad (2)$$

$$H = \rho_a c_p C_H u (\theta_s - \theta_a), \quad (3)$$

where ρ_a is air density, L_v is the latent heat of vapourization, c_p is the specific heat of air at constant pressure, u is horizontal wind speed at the reference height z , q_s and q_a are the specific humidity at the surface and the reference height, θ_s and θ_a are the potential temperature at the surface and the reference height. Here θ_s was obtained from the outgoing longwave radiation flux using the Stephan–Boltzmann law and with an emissivity of 0.97. Because the radiative skin temperature was used, our analysis avoided the cool-skin and warm-layer effects described by Fairall et al. (1996).

In Eqs. 1–3, C_D , C_E and C_H are the transfer coefficients for momentum, moisture and sensible heat, respectively, also referred to as the drag coefficient, Stanton number and Dalton number, respectively. They are related to the roughness lengths for momentum (z_m), water vapour (z_q) and heat (z_T) as

$$C_D = k^2 / [\ln(z/z_0) - \Psi_M(\zeta)]^2, \quad (4)$$

$$C_E = k^2 / \{[\ln(z/z_0) - \Psi_M(\zeta)][\ln(z/z_q) - \Psi_W(\zeta)]\}, \quad (5)$$

$$C_H = k^2 / \{[\ln(z/z_0) - \Psi_M(\zeta)][\ln(z/z_T) - \Psi_H(\zeta)]\}, \quad (6)$$

where k is the von Karman constant, Ψ_M and Ψ_H are the integral similarity functions for momentum and heat, respectively (Garratt 1992), and ζ is the Obukhov stability parameter.

Two approaches were used to determine the transfer coefficients. In the first approach, to quantify the variation of the transfer coefficients with wind speed, we first obtained C_D , C_H and C_E by inverting Eqs. 1–3 for each 30-min observation using the observed flux and the gradient variables. Next we computed the roughness lengths z_0 , z_q and z_T from Eqs. 4 to 6 with the appropriate stability correction. Finally we computed C_{D10N} , C_{E10N} and C_{H10N} according to

$$C_{D10N} = k^2 / [\ln(z/z_0)]^2, \quad (7)$$

$$C_{E10N} = k^2 / [\ln(z/z_0) \ln(z/z_q)], \quad (8)$$

$$C_{H10N} = k^2 / [\ln(z/z_0) \ln(z/z_T)], \quad (9)$$

with $z = 10$ m. These coefficients are for the standard reference height of 10 m and for neutral stability. The mean values and the standard deviations of these coefficients were calculated for each wind speed bin (bin width 1 m s^{-1}) consisting of 140–554 data points for the BFG site, 105–694 data points for the DPK site, and 108–687 data points for the MLW site.

In the second approach, we determined the “effective” transfer coefficients (C_{D10} , C_{E10} and C_{H10}) for each site using all the valid 30-min observations. We first adjusted the measured wind speed to the wind speed at the 10-m height using the standard logarithmic wind law. With the neutral stability assumption, u_{10} was calculated from the measured u_* and wind speed; the adjustment was small, on average 0.2, 0.1, and 0.5 m s^{-1} at the BFG, DPK and MLW sites, respectively. Next the coefficients were obtained from linear regression involving Eqs. 1–3. For example, the slope of the regression of the square of wind speed (at the 10-m height) versus the square of u_* is equivalent to C_{D10} according to Eq. 1. This method does not remove the effects of thermal stability nor relate the transfer coefficients to wind speed, but allows us to compare with values inferred from published studies that do not contain sufficient information on wind-speed and air-stability dependence.

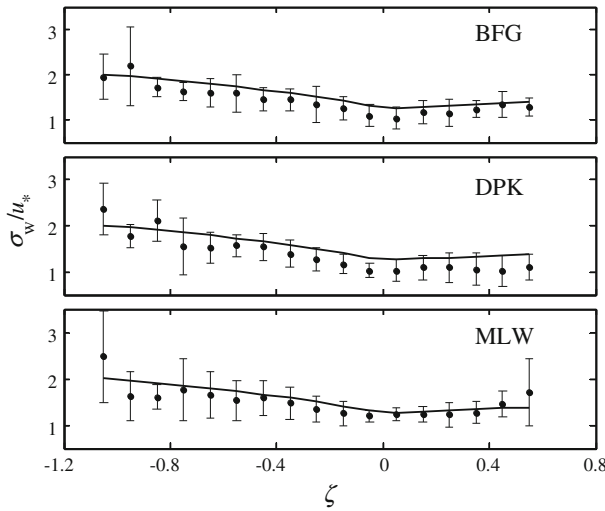


Fig. 3 Variation of σ_w/u_* with ζ of the measurement (dots) and the literature relationship. Error bars are one standard deviation of σ_w/u_* of each ζ bin (bin width 0.1) (solid line; Garratt 1992; Kaimal and Finnigan 1994)

3 Results and Discussion

3.1 Data Quality

The Monin–Obukhov scaling relationships can be used to determine whether the measurements suffer interference from the instrument-mounting hardware and the platform. Flow interference is a concern especially at the DPK and BFG sites where the measurement platform (3 m by 3 m at the DPK site and 5.5 m by 5.5 m at the BFG site) may have caused a bluff body effect on the otherwise undisturbed flow over the lake, possibly resulting in poor data quality. Here we compared the measurements with the established relationships between σ_w/u_* and ζ (Garratt 1992; Kaimal and Finnigan 1994)

$$\sigma_w/u_* = 1.25(1 - 3\zeta)^{1/3} \quad \text{for } \zeta < 0, \tag{10}$$

$$\sigma_w/u_* = 1.25(1 + 0.2\zeta) \quad \text{for } \zeta > 0, \tag{11}$$

where σ_w is the standard deviation of vertical wind speed, $\zeta = z/L$, and L is the Obukhov length. If there existed dynamic flow interference, we expect it to affect the σ_w , u_* and ζ measurements differently and the data to deviate significantly from Eqs. 10 and 11.

Figure 3 shows that the observed pattern of σ_w/u_* versus ζ agreed well with the relationship described by Eq. 10 in unstable conditions (with $\zeta < 0$) and Eq. 11 in stable conditions (with $\zeta > 0$). This result suggests that the interference of the measurement platform and the instrument-mounting hardware was negligible in the selected wind-direction range. The neutral σ_w/u_* value at the MLW site (1.21 ± 0.13) was in agreement with the standard neutral value of 1.25. At the BFG (1.04 ± 0.25) and DPK sites (1.01 ± 0.18) σ_w/u_* was smaller than the standard value. Smaller neutral values of σ_w/u_* have been reported in other field observations, such as over a dry lake bed (Wilson 2008), in a cattle range (Moraes 2000) and in flat fields with bare soil, grass and beans (Pahlow et al. 2001). The difference in the neutral stability value among the sites may have been related to differences in measurement

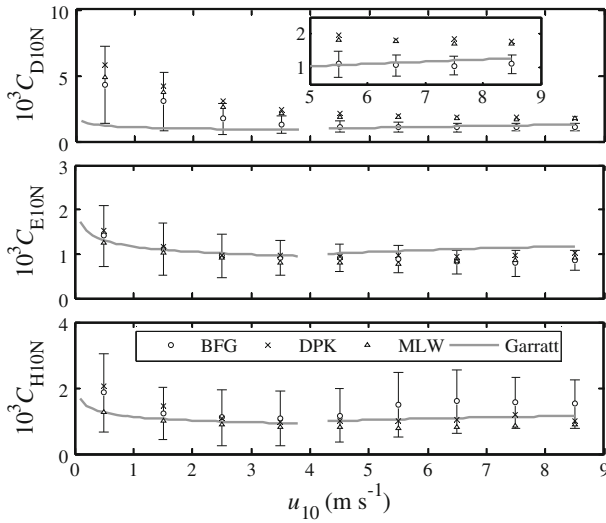


Fig. 4 Transfer coefficients at 10-m height (C_{D10N} , C_{E10N} and C_{H10N}) for the BFG (circles), DPK (crosses) and MLW (triangles) sites. Inset to the top panel an amplified plot for the wind-speed range 5–9 m s⁻¹. Error bars represent ± 1 standard deviation of the measurements at the BFG site (The standard deviations of the measurements at the MLW and DPK sites are similar to those at the BFG site)

height (3.54, 8.50, and 8.45 m at the MLW, DPK, and BFG sites, respectively). Another factor is flow interference by the larger measurement platforms at the DPK and BFG sites than at the MLW site, although it is not clear why aerodynamic inference should reduce σ_w more than u_* .

3.2 Effect of Submerged Vegetation

Both the wind-dependent neutral drag coefficient (Fig. 4) and the effective drag coefficients at the BFG site (Table 1; Fig. 5) were lower than at the DPK and MLW sites. We attribute this difference to the effect of submerged macrophytes at the BFG site. According to Fig. 4, the vegetation effect is also dependent on wind speed. It is well documented that submerged macrophytes influence the physical environment of the lake by decreasing light penetration, enhancing the strength of temperature stratification (Dale and Gillespie 1977), influencing re-suspension and sediment distribution (James and Barko 2000; Vermaat et al. 2000), and reducing turbulent mixing in the water (Herb and Stefan 2005) and the water flow velocity (Losee and Wetzel 1993; Barko and James 1998; Madsen et al. 2001). The BFG site was surrounded by submerged macrophytes (mainly *Potamogeton malaianus* and *Hydrilla verticillata*) (Fig. 2). The effective drag coefficient was 37 and 42 % lower than that at the MLW and DPK sites, respectively; the difference between the wind-dependent transfer coefficient in strong winds ($u_{10} > 4$ m s⁻¹) at the BFG site and those at the MLW and DPK sites was significant, at a confidence level of $p < 0.001$. For reference, the percentage of strong winds ($u_{10} > 4$ m s⁻¹) was 55, 62 and 43 % at the BFG, DPK and MLW sites, respectively, and the wind-speed histograms are shown in Fig. 6.

The effect of the submerged vegetation on the heat and water vapour transfer coefficients was less definite than that on the drag coefficient (Table 1; Fig. 5). The effective C_{E10} at the BFG site was nearly identical to that at the MLW and DPK sites, while the effective C_{H10}

Table 1 A summary of the effective transfer coefficients for momentum, moisture and heat calculated from the eddy-covariance measurements in lakes

Lake name	Location	Area (km ²)	Mean depth (m)	Maximum depth (m)	Data period	10 ³ CD10	10 ³ CE10	10 ³ CH10	References
Lake Taihu, China	31.17°N, 120.40°E (BFG site)	2,400	1.8	2.4	15 Dec 2011–30 Jun 2012	1.1 ± 0.02	1.0 ± 0.01	1.4 ± 0.02	This study
Lake Tännaren, Sweden	31.27°N, 119.93°E (DPK site)		2.6	3.1	18 Aug 2011–30 Jun 2012	1.9 ± 0.03	1.0 ± 0.01	1.2 ± 0.02	
Great Slave Lake, Canada	31.40°N, 120.22°E (MLW site)		1.9	2.5	14 Jun 2010–30 Jun 2012	1.8 ± 0.02	0.9 ± 0.01	1.5 ± 0.02	
Lake Valkea-Kotinen, Finland	61.23°N, 25.05°E	0.4	2.5	6.5	Apr–Oct, 2005–2008	5.2 ± 1.05	1.0 ± 0.04	1.0 ± 0.09	Nordbo et al. (2011)
Lake Tännaren, Sweden	60.00°N, 12.20°E	37	1.2	2	8–23 Jun 1994, 20 Jun–14 Jul 1995	1.4 ± 0.34	1.0 ± 0.40	1.3 ± 0.35	Heikinheimo et al. (1999)
Ross Rarnett Reservoir, Mississippi, USA	32.43°N, 90.03°W	134	5	8	1 Sep 2007–28 Feb 2008	1.7 ± 0.12	1.2 ± 0.06	1.1 ± 0.09	Liu et al. (2009)
Great Slave Lake, Canada	61.92°N, 113.73°W	27,000	41	614	Ice-free periods, 1997–1998	1.1 ± 0.06	2.0 ± 0.19	0.4 ± 0.05	Blanken et al. (2003)

The uncertainty range represents of 95 % confidence intervals for the coefficients estimates

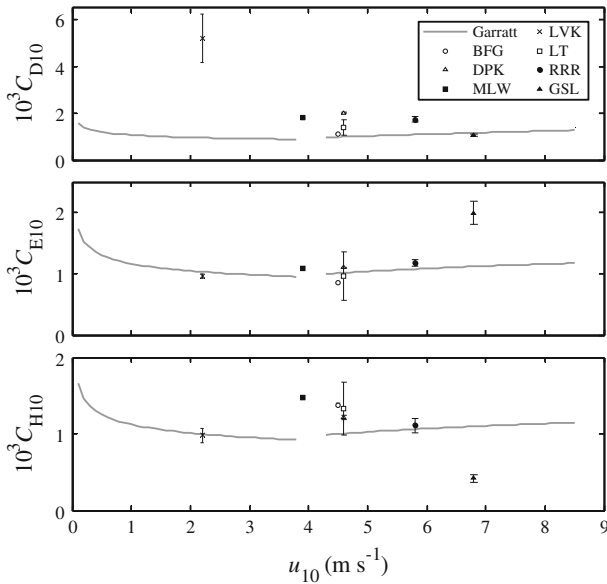


Fig. 5 Effective transfer coefficients at 10-m height (C_{D10} , C_{E10} and C_{H10}) versus the mean values of u_{10} for the lakes described in Table 1: *BFG* Bifenggang site in Lake Taihu, *DPK* Dapukou site in Lake Taihu, *MLW* Meiliangwan site in Lake Taihu, *LVK* Lake Valkea-Kotinen, *LT* Lake Tännaren, *RRR* Ross Rarnett Reservoir, *GSL* Great Slave Lake

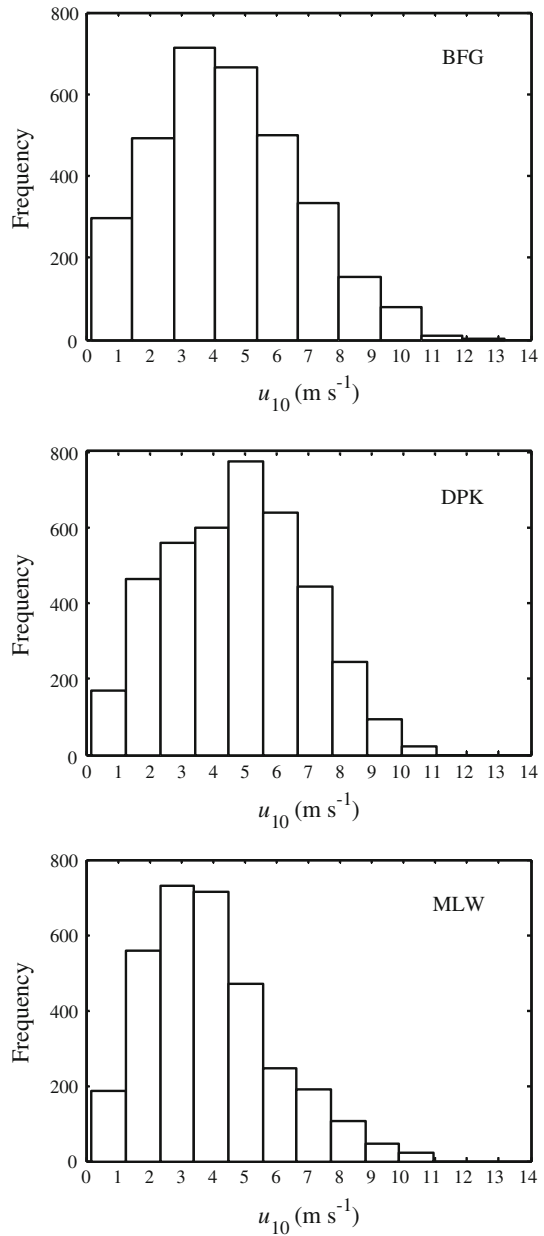
fell between the values at the MLW and DPK sites. That the drag coefficient is primarily controlled by form drag associated with surface roughness whereas the transfer coefficients are also dependent on the molecular diffusion resistance (Garratt 1992) may be the reason for the different responses of C_{D10} , C_{E10} and C_{H10} to the presence of submerged vegetation.

3.3 Wind Dependence

C_{D10N} at the three sites all showed a decreasing trend with increasing wind speed (Fig. 4, top panel). In the weak wind regime ($0-4 \text{ m s}^{-1}$), C_{D10N} decreased quickly with increasing wind speed, from 5.8×10^{-3} ($0 < u_{10} \leq 1 \text{ m s}^{-1}$) to 2.4×10^{-3} ($3 < u_{10} \leq 4 \text{ m s}^{-1}$) at the DPK site and from 4.8×10^{-3} ($0 < u_{10} \leq 1 \text{ m s}^{-1}$) to 1.7×10^{-3} ($3 < u_{10} \leq 4 \text{ m s}^{-1}$) at the MLW site. The extremely large C_{D10N} in low wind-speed conditions ($u_{10} < 1 \text{ m s}^{-1}$) may have been caused by rough capillary waves under these circumstances (Roll 1948; Zilitinkevich 1969; Foken 2008). Grachev et al. (1998) showed that the large C_{D10N} in low winds is partly an artifact of omitting gustiness in using the mean vector wind speed in the bulk parametrization. In strong winds, C_{D10N} decreased more slowly with increasing wind speed, reaching an asymptotic value of 1.8×10^{-3} at the DPK site and 1.7×10^{-3} at the MLW site when $u_{10} > 5 \text{ m s}^{-1}$. The asymptotic value at the BFG site was 1.1×10^{-3} .

High C_{D10N} values in low winds are attributed to the effect of viscous features of lake water. In low winds, the flow is aerodynamically smooth, and the roughness length is controlled by the viscous sublayer thickness, which is negatively correlated with u_* (Hinze 1975; Garratt 1992). In this regime, C_{D10N} should decrease with increasing wind speed. When flow is rough at high wind speeds, the drag coefficient becomes dependent on the surface roughness protuberances (waves) and should increase with increasing wind speed. That C_{D10N}

Fig. 6 Wind-speed histograms at the BFG, DPK and MLW sites



approached constant values in high winds (Fig. 4, top panel) suggests that, not surprisingly, wave development in Lake Taihu was hindered by its shallow depth. The median value of the wave height was 0.13, 0.18 and 0.12 m at the BFG, DPK and MLW sites, respectively, according to the empirical relation of [Davidan et al. \(1985\)](#). The transitional regime between aerodynamically smooth and rough flow is 2.5–5.5 m s^{-1} ([Garratt 1992](#)).

With abundant phytoplankton and no submerged macrophytes present at either the DPK or MLW site, the difference in C_{D10N} between the two sites may suggest an influence of

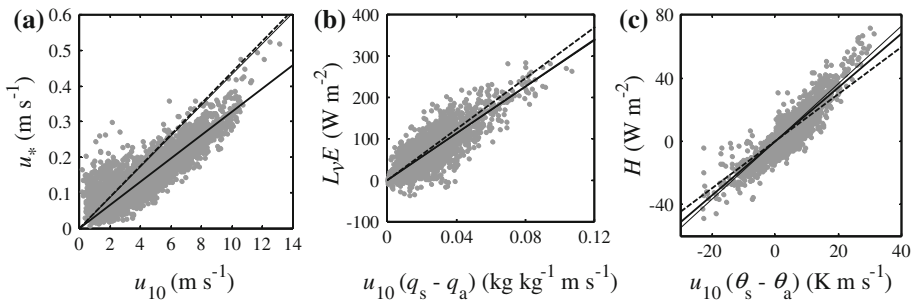


Fig. 7 Bulk transfer relationships at the three lake sites: **a** u_* versus u_{10} ; **b** $L_v E$ versus $u_{10}(q_s - q_a)$; **c** H versus $u_{10}(\theta_s - \theta_a)$. *dots* observations at the BFG site; *thick solid line* regression for the BFG site; *dashed line* regression for the DPK site; *thin solid line* regression for the MLW site. For clarity of presentation, data for the DPK and MLW sites are not shown. The data points are 0.5-h mean values

water depth. The DPK site was located in the deeper portion of the lake (water depth 2.6 m) whereas at the MLW site the water depth (1.9 m) was close to the mean depth of the lake. The difference was evident at low wind speeds (Fig. 4, top panel), with the DPK site having higher C_{D10N} than at the MLW site. The difference in the effective C_{D10} is negligibly small (1.9×10^{-3} at the DPK site versus 1.8×10^{-3} at the MLW site; Table 1).

Similar to C_{D10N} , C_{E10N} showed a decreasing trend with increasing wind speed although the rate of change was not as large as for C_{D10N} (Fig. 4, middle panel). In strong winds ($u_{10} > 5 \text{ m s}^{-1}$), C_{E10N} approached 0.9×10^{-3} at the BFG site, 1.0×10^{-3} at the DPK site and 0.9×10^{-3} at the MLW site.

C_{H10N} showed a decreasing trend with increasing wind speed in weak winds, varying in the range of 1.9×10^{-3} to 1.1×10^{-3} at the BFG site, from 2.1×10^{-3} to 1.0×10^{-3} at the DPK site, and from 2.1×10^{-3} to 1.3×10^{-3} at the MLW site (Fig. 4, bottom panel). In strong winds ($u_{10} > 5 \text{ m s}^{-1}$), C_{H10N} appears to show a slight increasing trend with increasing wind speed.

3.4 Comparison with Published Results

The effective transfer coefficients C_{D10} , C_{E10} and C_{H10} were calculated using the mass transfer relationships (Eqs. 1–3). The relationships of u_{10} versus u_* , $u_{10}(q_s - q_a)$ versus $L_v E$ and $u_{10}(\theta_s - \theta_a)$ versus H are shown in Fig. 7 for the BFG site. Part of the scatter was caused by variations in thermal stability and wind speed, but in general a linear regression provided a good fit to the data, explaining 79, 75 and 82% of the observed variations in u_* , $L_v E$ and H , respectively. Similar results were obtained for the MLW and DPK sites. The transfer coefficients determined from the slope of the regression are summarized in Table 1. The most important result is the low momentum transfer or drag coefficient C_{D10} at the BFG site in comparison to those at the DPK and MLW sites, which is consistent with the results shown in Fig. 4 (top panel).

In Table 1, the effective transfer coefficients for Lake Taihu are compared with the values inferred from the published studies for four other freshwater lakes, including Lake Valkeakotinen (Nordbo et al. 2011), Lake Tämnen (Heikinheimo et al. 1999), Ross Barnett Reservoir (Liu et al. 2009) and Great Slave Lake (Blanken et al. 2003). In Blanken et al. (2003); Liu et al. (2009) and Nordbo et al. (2011), the flux data are presented in the forms similar to Fig. 7, and the effective transfer coefficients were derived from the slope of their data plots.

In Heikinheimo et al. (1999), C_D , C_E and C_H at 3-m height are given for different stability conditions, and we used the mean value of their data and corrected to the 10-m height. Table 1 shows that C_{D10} ranges from 1.1×10^{-3} to 5.2×10^{-3} , C_{E10} from 1.0×10^{-3} to 2.0×10^{-3} , and C_{H10} from 0.4×10^{-3} to 1.5×10^{-3} . The mean (standard deviation) value of C_{D10} , C_{E10} and C_{H10} for the five lakes is $2.0 (\pm 1.4) \times 10^{-3}$, $1.1 (\pm 0.4) \times 10^{-3}$ and $1.1 (\pm 0.4) \times 10^{-3}$, respectively. The effective C_{D10} at the BFG site (with a value of 1.1×10^{-3}) was significantly lower than the mean C_{D10} value.

In a related study, Sheppard et al. (1972) reported that for a deep lake (Lough Neagh) in Northern Ireland, the effective drag coefficient increased linearly with wind speed from 0.7×10^{-3} at a wind speed of 3 m s^{-1} to 2.0×10^{-3} at a wind speed of 16 m s^{-1} . The values in Table 1 fall within their data range, although here the effective drag coefficient shows a reverse trend with wind speed (see below).

Lake physical characteristics seem to have some impact on the transfer coefficients. C_{E10} is positively correlated with water depth; the linear correlation is $r = 0.94$ ($p < 0.01$) if the Great Slave Lake is excluded, and is $r = 0.99$ ($p < 0.001$) if it is included. C_{E10} is also correlated with lake area ($r = 0.96$, $p < 0.01$; including the Great Slave Lake). On the other hand C_{H10} is negatively correlated with water depth ($r = -0.84$, $p < 0.05$) and lake area ($r = -0.90$, $p < 0.01$). The correlation of C_{D10} with lake depth ($r = -0.30$, $p > 0.50$) and size ($r = -0.35$, $p > 0.40$) is not significant. Panin et al. (2006) showed that the sensible and latent heat fluxes are enhanced by shallow depth, but our comparison shows that the water vapour transfer coefficient was lower for shallower lakes. In high turbulent flow, fetch tends to limit wave development and reduce the transfer coefficients (Donelan et al. 1993; Maat et al. 1991; Smith et al. 1992; Vickers and Mahrt 1997; Subin et al. 2012). Our literature survey suggests that fetch or lake size influence C_{E10} , C_{H10} and C_{D10} differently. The disagreement with the theoretical expectation may have been caused by the fact that air stability was different among the lake studies we examined.

Figure 5 shows the dependence of the effective transfer coefficients on wind speed. There is a significantly negative correlation between u_{10} and C_{D10} , and no correlation is seen for C_{E10} and C_{H10} . The correlation coefficient between C_{D10} and u_{10} is $r = -0.79$ ($p < 0.05$) with the Great Slave Lake included and $r = -0.83$ ($p < 0.05$) with the Great Slave Lake excluded. The low value of C_{D10} for Lake Tämnaaren (1.4×10^{-3}) may be indicative of the influence of aquatic vegetation as there were reeds and water lilies in the water near the shoreline of Lake Tämnaaren (Wallsten and Forsgren 1989). Theoretically, increasing wind speed should enhance the transfer coefficients through increasing wave height in the high wind or high turbulent regime (Davidan et al. 1985), and should decrease roughness length in aerodynamically smooth flow or in the low wind regime (Fairall et al. 1996). Our study neither supports nor contradicts this relation, since the wind speed over the lakes considered in this study (with mean u_{10} ranging from 2.2 to 6.8 m s^{-1}) fell in the transitional regime between aerodynamically smooth and rough flow (2.5 – 5.5 m s^{-1}).

3.5 Comparison with Model Parametrizations

In Garratt (1992), separate C_{D10N} , C_{H10N} and C_{E10N} parametrizations are given for smooth and rough flow (Fig. 4). In smooth flow, the momentum and scalar roughness are controlled by the viscous force and molecular diffusion in the interfacial air layer of the water surface (Zilitinkevich 1969). In rough flow, the momentum roughness is related to wave development according to Charnock's model and the scalar roughness is a weak function of the roughness

Reynolds number. The rough flow parametrizations are shown to agree with observational data over sea surfaces (Garratt 1992).

At Lake Taihu, the modelled C_{D10N} , C_{E10N} and C_{H10N} were biased low in low winds ($u_{10} < 2 \text{ m s}^{-1}$) at all three sites. In high winds ($u_{10} > 5 \text{ m s}^{-1}$), good agreement in C_{D10N} was found for the BFG site and high bias (by 26–44 %) at the DPK and MLW sites. The modelled C_{E10N} was biased high by 4–33 % at the three sites when $u_{10} > 5 \text{ m s}^{-1}$. The modelled C_{H10N} was in agreement with the observations at the DPK site and was biased high (by 14–27 %) at the MLW and BFG sites when $u_{10} > 5 \text{ m s}^{-1}$.

The model parametrizations are also compared with the effective transfer coefficients (Fig. 7). The results are broadly consistent with the comparison of the neutral values (Fig. 4). Significantly low bias in C_{D10} was found for Lake Valkea-Kotinen with a low u_{10} value of 2.2 m s^{-1} . For the other lake experiments at higher wind speeds ($u_{10} > 3.5 \text{ m s}^{-1}$), the bias was much reduced (mean bias -27%). Large biases in C_{E10} and C_{H10} occurred at the Great Slave Lake with a high u_{10} value of 6.8 m s^{-1} ; these biases may have been caused by the heat exchange due to spray and droplet evaporation at high wind speeds (Deacon 1977). Excluding the Great Slave Lake data, the disagreement in C_{E10} and C_{H10} falls within the range of the parametrization and the measurement uncertainties.

The comparison between the observational data and the model parametrization suggests that at the same wind speed, the water surface of a lake is rougher than the ocean surface except when submerged vegetation is present. The predicted increase in C_{D10N} with increasing wind speed in rough flow is not evident in the data.

The results presented here are broadly consistent with the study by Grachev et al. (2011). Using ship-based measurements, they showed that the momentum flux calculated with the COARE bulk parametrization is in agreement with the observed flux in the open ocean (Gulf of Mexico). But when compared with measurements over shallower water (bays, lakes, coastal harbours), the same parametrization shows a low bias by as much as a factor of 4 under light wind conditions ($u_* < 0.2 \text{ m s}^{-1}$, or $u_{10} < 4 \text{ m s}^{-1}$). Interestingly, the computed sensible heat and latent heat fluxes are in good agreement with the observations in both situations. The percentage of weak winds ($u_{10} < 4 \text{ m s}^{-1}$) was around 50 % in the observations at the three sites in Lake Taihu (Fig. 6), so the low wind regime cannot be ignored.

4 Conclusions

Eddy-covariance systems were used to measure the momentum, heat and water vapour fluxes at three sites in Lake Taihu, China. Two of these sites were in water free of macrophytes and one was surrounded by submerged macrophytes. Wind-dependent and effective bulk transfer coefficients were calculated based on the observations. The key findings are:

- (1) The effective momentum transfer coefficient (approximated by the slope of the regression of u_*^2 against u_{10}^2) was reduced by approximately 40 % in the presence of submerged macrophytes.
- (2) At all three Lake Taihu sites, the drag coefficient and the transfer coefficients of moisture and heat under neutral stability were wind dependent, with a decreasing trend with increasing wind speed for weak winds ($u_{10} < 4 \text{ m s}^{-1}$). They approached constant values in strong winds ($u_{10} > 4 \text{ m s}^{-1}$), indicating that wave growth was retarded by the shallow depth of the lake (mean lake depth 1.9 m).
- (3) The mean (standard deviation) values of the effective drag and transfer coefficients C_{D10} , C_{E10} and C_{H10} are $2.0 (\pm 1.4) \times 10^{-3}$, $1.1 (\pm 0.4) \times 10^{-3}$ and $1.1 (\pm 0.4) \times 10^{-3}$, respectively, according to our observations and published studies for other lakes.

- (4) At the MLW and DPK sites (free of submerged macrophytes), the observed C_{D10N} was higher than the prediction according to the Garratt (1992) model for the marine environment. At a wind speed $u_{10} = 8.5 \text{ m s}^{-1}$, the difference is about 35%. It appears that at the same wind speed, the water surface of the lake was rougher than the ocean surface.

Our study suggests that the transfer coefficients taken from experimental studies conducted in the open oceans may be subject to large uncertainties when applied to inland lakes, especially in the presence of submerged macrophytes or if the lake is shallow and wind speed is low. Land-surface models used in numerical weather prediction and climate models appear sensitive to the transfer coefficient parametrizations. For example, in a sensitivity analysis using the NCAR lake model, we have showed previously that the adoption of the observed transfer coefficients improves the prediction of the lake surface temperature and sensible and latent heat fluxes (Deng et al. 2013).

Acknowledgments This research was supported by the Natural Science Foundation of Jiangsu Province, China (grant BK2011830), the Ministry of Education of China (grant PCSIRT), the Priority Academic Program Development of Jiangsu Higher Education Institutions (grant PAPD) and the National Natural Science Foundation of China (grant 41275024). We thank three reviewers whose constructive comments have improved this paper.

References

- Ataktürk SS, Katsaros KB (1999) Wind stress and surface waves observed on Lake Washington. *J Phys Oceanogr* 29:633–650
- Barko JW, James WJ (1998) Effects of submerged aquatic macrophytes on nutrient dynamics, sedimentation, and resuspension. In: Jeppesen E et al (eds) *The structuring role of submerged macrophytes in lakes*. Springer, New York, pp 197–214
- Blanken PD, Rouse WR, Culf AD, Spence C, Boudreau LD, Jasper JN, Kochtubajda B, Schertzer WM, Marsh P, Versegny D (2000) Eddy covariance measurements of evaporation from Great Slave Lake, Northwest Territories, Canada. *Water Resour Res* 36:1069–1077
- Blanken PD, Rouse WR, Schertzer WM (2003) Enhancement of evaporation from a large northern lake by the entrainment of warm, dry air. *J Hydrometeorol* 4:680–693
- Blanken PD, Spence C, Hedstrom N, Lenters JD (2011) Evaporation from Lake Superior: 1. Physical controls and processes. *J Great Lakes Res* 37:707–716
- Carpenter SR, Lodge DM (1986) Effects of submersed macrophytes on ecosystem processes. *Aquat Bot* 26:341–370
- Chen Y, Qin B, Teubner K, Dokulil MT (2003) Long-term dynamics of phytoplankton assemblages: Microcystis-domination in Lake Taihu, a large shallow lake in China. *J Plankton Res* 25:445–453
- Dale HM, Gillespie TJ (1977) The influence of submersed aquatic plants on temperature gradients in shallow water bodies. *Can J Bot* 55:2216–2225
- Davidan IN, Lopatuhin LI, Rozhkov VA (1985) *Waves in the world ocean* (in Russian). *Gidrometeoizdat, Leningrad*, p 256
- Deacon EL (1977) Gas transfer to and across an air–water interface. *Tellus* 29:363–374
- Deng B, S Liu, W Xiao, W Wang, J Jin, X Lee (2013) Evaluation of the CLM4 lake model at a large and shallow freshwater lake. *J Hydrometeorol* 14:636–649
- Donelan MA, Dobson FW, Smith SD, Anderson RJ (1993) On the dependence of sea-surface roughness on wave development. *J Phys Oceanogr* 23:2143–2149. doi:10.1175/1520-0485(1993)023<2143:OTDOSS>2.0.CO;2
- Downing JA, Prairie YT, Cole JJ, Duarte CM, Tranvik LJ, Striegl RG, McDowell WH, Kortelainen P, Caraco NF, Melack JM, Middelburg JJ (2006) The global abundance and size distribution of lakes, ponds, and impoundments. *Limnol Oceanogr* 51:2388–2397
- Fairall CW, Bradley EF, Godfrey JS, Wick GA, Edson JB, Young GS (1996) Cool-skin and warm-layer effects on the sea surface temperature. *J Geophys Res* 101:1295–1308
- Foken T (2008) *Micrometeorology*. Springer, Berlin

- Gao ZQ, Wang Q, Zhou MY (2009) Wave-dependence of friction velocity, roughness length, and drag coefficient over coastal and open water surfaces by using three databases. *Adv Atmos Sci* 26:887–894
- Garratt JR (1992) The atmospheric boundary layer. Cambridge University Press, Cambridge
- Geernaert GL, Larsen SE, Hansen F (1987) Measurements of the wind-stress, heat-flux and turbulence intensity during storm conditions over the north sea. *J Geophys Res* 92:13127–13139
- Grachev AA, Fairall CW, Larsen SE (1998) On the determination of the neutral drag coefficient in the convective boundary layer. *Boundary-Layer Meteorol* 86:257–278
- Grachev AA, Bariteau L, Fairall CW, Hare JE, Helmig D, Hueber J, Lang EK (2011) Turbulent fluxes and transfer of trace gases from ship-based measurements during TexAQS 2006. *J Geophys Res* 116:D13110
- Heikinheimo M, Kangas M, Tourula T, Venäläinen A, Tattari S (1999) Momentum and heat fluxes over lakes Tämnen and Råksjö determined by the bulk-aerodynamic and eddy-correlation methods. *Agric For Meteorol* 98–99:521–534
- Henderson-Sellers B (1986) Calculating the surface energy balance for lake and reservoir modeling: A review. *Rev Geophys* 24:625–649
- Herb WR, Stefan HG (2005) Dynamics of vertical mixing in a shallow lake with submersed macrophytes. *Water Resour Res* 41:W02023. doi:[10.1029/2003WR002613](https://doi.org/10.1029/2003WR002613)
- Hinze JO (1975) Turbulence: an introduction to its mechanism and theory, 2nd edn. McGraw-Hill, New York
- Hsieh CI, Katul G, Chi T (2000) An approximate analytical model for footprint estimation of scalar fluxes in thermally stratified atmospheric flows. *Adv Water Resour* 23:765–772
- James WF, Barko JW (2000) Sediment resuspension dynamics in canopy- and meadow-forming submersed macrophyte communities. Rep ERDC/EL SR-00-8, US Army Corps of Engineers, Vicksburg, Miss, USA, 38 pp
- Johnson RK, Ostrofsky ML (2004) Effects of sediment nutrients and depth on small-scale spatial heterogeneity of submersed macrophyte communities in Lake Pleasant, Pennsylvania. *Can J Fish Aquat Sci* 61:1493–1502
- Kaimal JC, Finnigan JJ (1994) Atmospheric boundary layer flows: their structure and measurement. Oxford University Press, New York
- Lee X, Massman W (2011) A perspective on thirty years of the Webb, Pearman and Leuning density corrections. *Boundary-Layer Meteorol* 139:37–59. doi:[10.1007/s10546-010-9575-z](https://doi.org/10.1007/s10546-010-9575-z)
- Lee X, Massman W, Law B (2004) Handbook of micrometeorology: a guide for surface flux measurement and analysis. Kluwer, Dordrecht
- Liu H, Randerson JT, Lindfors J, Chapin III FS (2005) Changes in the surface energy budget after fire in boreal ecosystems of interior Alaska: an annual perspective. *J Geophys Res* 110:D13101. doi:[10.1029/2004JD005158](https://doi.org/10.1029/2004JD005158)
- Liu H, Zhang Y, Liu S, Jiang H, Sheng L, Williams QL (2009) Eddy covariance measurements of surface energy budget and evaporation in a cool season over southern open water in Mississippi. *J Geophys Res* 114:D04110. doi:[10.1029/2008JD010891](https://doi.org/10.1029/2008JD010891)
- Losee RF, Wetzel RC (1993) Littoral flow rates within and around submersed macrophyte communities. *Freshwater Biol* 29:7–17
- MacKay MD, Neale PJ, Arp CD, De Senerpont Domis LN, Fang X, Gal G, Jöhnk KD, Kirillin G, Lenters JD, Litchman E, MacIntyre S, Marsh P, Melack J, Mooij WM, Peeters F, Quesada A, Schladow SG, Schmid M, Spence C, Stokes SL (2009) Modeling lakes and reservoirs in the climate system. *Limnol Oceanogr* 54:2315–2329
- Madsen JD, Chambers PA, James WF, Koch EW, Westlake DF (2001) The interaction between water movement, sediment dynamics and submersed macrophytes. *Hydrobiologia* 444:71–84
- Matt N, Kraan C, Oost WA (1991) The roughness of wind-waves. *Boundary-Layer Meteorol* 54:89–103. doi:[10.1007/BF00119414](https://doi.org/10.1007/BF00119414)
- Moraes OLL (2000) Turbulence characteristics in the surface boundary layer over the South American pampa. *Boundary-Layer Meteorol* 96:317–335
- Nepf HM (1999) Drag, turbulence, and diffusion in flow through emergent vegetation. *Water Resour Res* 35:479–489
- Nordbo A, Launiainen S, Mammarella I, Leppäranta M, Huotari J, Ojala A, Vesala T (2011) Long-term energy flux measurements and energy balance over a small boreal lake using eddy covariance technique. *J Geophys Res* 116:D02119. doi:[10.1029/2010JD014542](https://doi.org/10.1029/2010JD014542)
- Oleson KW, Dai Y, Bonan G, Bosilovich M, Dickinson R, Dirmeyer P, Hoffman F, Houser P, Levis S, Niu G, Thornton P, Vertenstein M, Yang Z, Zeng X (2004) Technical description of the Community Land Model (CLM). NCAR Technical Note: NCAR/TN-461+STR. National Center for Atmospheric Research, Boulder, Colorado, USA, p 174
- Pahlow M, Parlange M, Porté-Agel F (2001) On Monin–Obukhov similarity in the stable atmospheric boundary layer. *Boundary-Layer Meteorol* 99:225–248

- Panin GN, Nasonov AE, Foken Th, Lohse H (2006) On the parameterisation of evaporation and sensible heat exchange for shallow lakes. *Theor Appl Climatol* 85:123–129. doi:[10.1007/s00704-005-0185-5](https://doi.org/10.1007/s00704-005-0185-5)
- Pip E (1979) Survey of the ecology of submerged aquatic macrophytes in central Canada. *Aquat Bot* 7:339–357
- Plew DR, Cooper GG, Callaghan FM (2008) Turbulence-induced forces in a freshwater macrophyte canopy. *Water Resour Res* 44:W02414. doi:[10.1029/2007WR006064](https://doi.org/10.1029/2007WR006064)
- Radomski P, Perleberg D (2012) Application of a versatile aquatic macrophyte integrity index for Minnesota lakes. *Ecol Indic* 20:252–268. doi:[10.1016/j.ecolind.2012.02.012](https://doi.org/10.1016/j.ecolind.2012.02.012)
- Roll HU (1948) Wassernahes windprofil und wellen auf dem wattenmeer. *Ann Meteorol* 1:139–151
- Rouse WR, Blanken PD, Bussi eres N, Oswald CJ, Schertzer WM, Spence C, Walker AE (2008) An investigation of the thermal and energy balance regimes of Great Slave and Great Bear Lakes. *J Hydrometeorol* 9:1318–1333. doi:[10.1175/2008JHM977.1](https://doi.org/10.1175/2008JHM977.1)
- Samuelsson P, Tjernstr om M (2001) Mesoscale flow modification induced by land-lake surface temperature and roughness differences. *J Geophys Res* 106D:12419–12435
- Samuelsson P, Kourzeneva E, Mironov D (2010) The impact of lakes on the European climate as simulated by a regional climate model. *Boreal Environ Res* 15:113–129
- Schertzer WM, Rouse WR, Blanken PD, Walker AE (2003) Over-lake meteorology and estimated bulk heat exchange of Great Slave Lake in 1998 and 1999. *J Hydrometeorol* 4:649–659
- Sheppard PA, Tribble DT, Garratt JR (1972) Studies of turbulence in the surface layer over water (Lough Neagh). Part I. Instrumentation, programme, profiles. *Q J R Meteorol Soc* 98:627–641
- Sills DML, Brook JR, Levy I, Makar PA, Zhang J, Taylor PA (2011) Lake breezes in the southern Great Lakes region and their influence during BAQS-Met 2007. *Atmos Chem Phys* 11:7955–7973
- Smith SD, Anderson RJ, Oost WA, Kraan C, Maat N, DeCosmo J, Katsaros KB, Davidson KL, Bumke K, Hasse L, Chadwick HM (1992) Sea-surface wind stress and drag coefficients: the HEXOS results. *Boundary-Layer Meteorol* 60:109–142. doi:[10.1007/BF00122064](https://doi.org/10.1007/BF00122064)
- S ndergaard M, Phillips G, Hellsten S, Kolada A, Ecke F, M emets H, Mjelde M, Azzella MM, Oggioni A (2013) Maximum growing depth of submerged macrophytes in European lakes. *Hydrobiologia* 704:165–177. doi:[10.1007/s10750-012-1389-1](https://doi.org/10.1007/s10750-012-1389-1)
- Subin ZM, Riley WJ, Mironov DV (2012) An improved lake model for climate simulations: model structure, evaluation, and sensitivity analyses in CESM1. *JAMES* 4:M02001
- T rnblom K, Bergstr om H, Jahansson C (2007) Thermally driven mesoscale flows—simulations and measurements. *Boreal Environ Res* 12:623–641
- Vermaat JE, Santamaria L, Roos PJ (2000) Water flow across and sediment trapping in submerged macrophyte beds of contrasting growth form. *Arch Hydrobiol* 148:549–562
- Vesala T, Huotari J, Rannik  , Suni T, Smolander S, Sogachev A, Launiainen S, Ojala A (2006) Eddy covariance measurements of carbon exchange and latent and sensible heat fluxes over a boreal lake for a full open-water period. *J Geophys Res* 111:D11101. doi:[10.1029/2005JD006365](https://doi.org/10.1029/2005JD006365)
- Vikers D, Mahrt L (1997) Fetch limited drag coefficients. *Boundary-Layer Meteorol* 85:53–79. doi:[10.1023/A:1000472623187](https://doi.org/10.1023/A:1000472623187)
- Wallsten M, Forsgren P (1989) The effects of increased water level on aquatic macrophytes. *J Aquat Plant Manag* 27:32–37
- Webb EK, Pearman GI, Leuning R (1980) Correction of flux measurements for density effects due to heat and water vapour transfer. *Q J R Meteorol Soc* 106:85–100
- Wilson JD (2008) Monin–Obukhov functions for standard deviations of velocity. *Boundary-Layer Meteorol* 129:353–369. doi:[10.1007/s10546-008-9319-5](https://doi.org/10.1007/s10546-008-9319-5)
- Zhao L, Jin J, Wang SY, Ek MB (2012) Integration of remote-sensing data with WRF to improve lake-effect precipitation simulations over the Great Lakes region. *J Geophys Res* 117:D09102. doi:[10.1029/2011JD016979](https://doi.org/10.1029/2011JD016979)
- Zilitinkevich SS (1969) On the computation of the basic parameters of the interaction between the atmosphere and the ocean. *Tellus* 21:17–24